Novel Poly(*n*-Butyl Methacrylate)/Titanium Oxide Alloys Produced by the Sol–Gel Process for Titanium Alkoxides

K. A. MAURITZ,* *Department of Polymer Science, University of Southern Mississippi, Southern Station Box 10076, Hattiesburg, Mississippi 39406-0076,* and C. K. JONES, *Exxon Research and Engineering Co., Clinton Township, Rte. 22 East, Annandale, New Jersey 08801*

Synopsis

A method has been developed to cast novel organic/inorganic hybrid films from multicomponent solutions containing titanium alkoxides, poly(*n*-butyl methacrylate), water, and isopropanol of prescribed compositions. The sol–gel reactions and controlled drying procedure yielded materials of mechanical integrity for which the multistep thermal degradation profile of the organic polymer has been significantly modified. A crystallization exotherm, presumably due to anatase formation, is seen for tetraethyl titanate-derived films beyond the organic degradation temperature. The trend of mechanical tensile parameters with increasing Ti oxide content depicts progressive material strengthening. FT-IR as well as the thermal and mechanical studies of these films suggest a highly unconnected and heterogeneous Ti oxide phase.

INTRODUCTION

There has been considerable interest in the low-temperature synthesis of inorganic glasses from metal alkoxides [$M(OR)_{3,4}$; M = Si, Ti, Zr, Al, R = methyl through butyl, usually] by the sol–gel process.[1–3] These alkoxides are readily soluble in lower alcohols, and when water is added to these solutions hydrolysis followed by polyfunctional condensation polymerization results in a three-dimensional network or gel. Hydrolysis–condensation rates are affected by acid, base, or soluble salt additions more so than by temperature or concentration, and the physical nature of the resultant gel is profoundly determined by drying conditions.[2,4,5]

It was the goal of this work to create and characterize novel solid mixtures of linear organic polymers and three-dimensional metal oxide networks. Consider an organic polymer that is totally soluble in a metal alkoxide/alcohol solution. Mutual solubility, of course, implies mixing of the components at the molecular level. A basic working hypothesis in these studies was that, following the completed sol–gel reaction after the addition of hydrolysis water and controlled drying, there may be an opportunity to derive an end composition that is in itself intimately mixed. One might think of a true *solid solution* in which the dispersed organic chains exist in single isolation in a continuous inorganic phase or at most in low-level aggregates that are still within the scale of mo-

* To whom requests for reprints should be sent.

Journal of Applied Polymer Science, Vol. 40, 1401–1420 (1990)
 CCC 0021-8995/90/07-81401-20$04.00

lecular dimensions at appropriately low organic polymer concentrations. On the other hand, at comparatively higher organic polymer concentrations, the condensed metal oxide phase might be dispersed into small, i.e., nanometers in size, domains, yielding a *microcomposite,* or into a fine *interpenetrating filamentary network.* Of course, the precise name chosen for the affected organic/inorganic hybrid materials should result from an unambiguous microstructural characterization. We have at least tentatively chosen to refer to our materials as "alloys" as this term, borrowed from the discipline of metallurgy, refers to large-scale molecular mixing but also allows for a degree of compositional segregation.[6]

Mark and co-workers have affected the *in situ* growth of 150–250 Å in diameter silica particles by the sol–gel reaction for tetraethoxysilane (TEOS) within poly(dimethylsiloxane).[7] Similar results have been achieved with poly(methyl phenylsiloxane) and polyisobutylene elastomers.[7] It is a practical goal in the area of elastomers to provide strong internal mechanical reinforcement by incorporating high surface/volume interactive fillers.[8,9] Conventional filler blending occurring under high-viscosity conditions, however, usually leads to particle agglomeration that diminishes polymer–filler interactions. Mark et al. affected particle in-growths with relatively narrow size distributions and no aggregation.[10,11] The tensile moduli and ultimate tensile strengths increased, and maximum extensibilities decreased with increasing silica filler content.[12]

Mauritz et al. have tailored the *in situ* growth of Si oxide microclusters and interpenetrating networks in perfluorosulfonic acid membranes via the sol–gel reaction for TEOS.[13–15] The existing polar/nonpolar phase-separated morphology of the unfilled polymer matrix was hypothesized to strongly direct the morphology of the resultant *in situ* inorganic phase by having various quantities of sorbed TEOS/alcohol/water solutions preferentially pool within the approximately 40 Å in diameter polar clusters. The ensuing TEOS hydrolysis within these cluster "microreactors" is conveniently catalyzed by the fixed SO_3H groups. Tensile properties vs. solids uptake indicated an initial strengthening, followed by a ductile-brittle transition suggesting a Si oxide phase percolation threshold. FT-IR and ^{29}Si solid-state NMR analyses of microstructural evolution portray an invasive inorganic network that is not as highly crosslinked as that of sol–gel-derived free silica and actually becomes less coordinated and less connected with increasing solids uptake.

Aside from obvious chemical differences, the outstanding process and before–after material distinctions between our earlier efforts and the work reported herein are as follows. In the former case the intrinsically slower sol–gel reaction (i.e., involving a Si vs. Ti alkoxide) is highly controlled by alkoxide diffusion into a pre-swollen insoluble semicrystalline polymer having the potential for sequestering reactants within a distinct isolated phase (with attached catalyst) that, in effect, serves as a three-dimensional template that directs the final spatial organization of the inorganic phase. In the present work, all initial components are cosoluble, and there is a more ambiguous basis for predicting the resultant morphologies of the dried films.

Wilkes et al.[16] created novel hybrid systems by adding titanium isopropoxide to preformed TEOS-derived gels in which functionalized *oligomers* of either poly(tetramethylene oxide) (PTMO) or poly(dimethylsiloxane) (PDMS) were trapped. In this procedure, the partial hydrolysis of TEOS and of the tetraeth-

oxysilane endcaps of PTMO were affected by the controlled release of water from an ongoing esterification of glacial acetic acid and isopropanol that are present in the solution. No water is directly added in this scheme. The silanol endgroups of the PDMS molecules can also participate in subsequent condensation reactions. Titanium isopropoxide is added later, and finally the system is gently heated to coax this complex sol–gel reaction to completion. It is claimed that these materials have compositional homogeneity on a scale smaller than the wavelength of light.[17,18]

Earlier, Wilkes and co-workers reported the incorporation of PDMS oligomers terminated with silanol groups into a TEOS-derived network.[19–22] These materials, dubbed "ceramers," exhibited a very local PDMS aggregation that could, however, be dispersed with initial acid addition as indicated by SAXS, dynamic mechanical, and solid-state NMR studies.

EXPERIMENTAL

Sample Preparation

Tetraethyl titanate (TET) and tetrabutyl titanate (TBT) liquids were donated by Kay Fries Co., and poly(n-butyl methacrylate) (PnBM) samples (M_n = 73,500, M_w/M_n = 4.35) were obtained from Aldrich Co., both being used as received.

Two grams of PnBM were added to 7.0 mL of isopropanol and stirred at 25°C in six sealed vials. After solubilization, six ternary solutions were made by adding 1, 2, or 3 mL of either TET or TBT to the polymer solutions. For the sake of brevity, we will refer to these final solutions as 1E, 2E, 3E, 1B, 2B, and 3B, respectively. Thus, for example, 2B refers to the ternary solution having 2 mL of TBT.

The titanate : butyl methacrylate repeat unit mole ratios for these solutions are listed in Table I. While the titanate component is always stoichiometrically less than or equal to the number of polymer chemical repeat units, the magnitudes are comparable, that is, neither component exists in dilution. Also, the mole ratios for the B series are, of course, correspondingly lower than those for the E series. We have calculated these ratios, based upon the densities of the liquid alkoxides (TET: 1.10 g/cm^3, TBT: 0.998 g/cm^3) to aid in the rationalization of our physical characterization results.

These solutions were cast onto clean glass substrates and then drawn to a 0.009 in. thickness in a controlled humidity (60% RH) enclosure to affect limited alkoxide hydrolysis in controlled fashion. The films were removed from the substrates after 3 min and placed in a vacuum oven at 130°C for 2 h to remove

TABLE I
Tetra(Ethyl, Butyl) Titanate : Butyl Methacrylate Repeat Unit Mole Ratios for Alkoxide/PnBM/Isopropanol Solutions

1E	2E	3E	1B	2B	3B
0.34	0.68	1.03	0.21	0.42	0.62

residual water and alcohol and drive unreacted Ti–OH groups to condensation within the polymer. The films were continuously stored in a desiccator prior to characterization studies.

At this point we will briefly mention that this procedure was also applied to solutions in which the alkoxide was either tetrabutyl zirconate or tetraisopropyl titanate, but highly fractured films of nonuniform thickness resulted in each case.

Film Characterization

Thermal transitions and corresponding progressive weight loss for these materials, upon heating at 10°C/min, were monitored using the differential scanning calorimetry (DSC) and thermogravimetric analysis (TGA) capabilities of the DuPont 9900 Thermal Analysis System. For the DSC studies, hermetically sealed aluminum pans were prepared to enclose all samples. These samples, of approximately 3 mg, were shaped to fit the bottom pan surfaces. A dynamic nitrogen atmosphere (500 mL N_2/min) flowed into the cell chamber for the duration of the scans that were run from 25–500°C. Samples used for TGA weighed approximately 5 mg and were placed in a platinum pan exclusively. This pan was flamed momentarily after each scan to ensure removal of residual materials. A 500 mL/min flow of nitrogen was introduced during operation to sweep generated volatiles.

The mechanical tensile properties of these films were determined with an Instron Model 1130. A high-impact compression stamp was used to produce samples of constant length and width. Crosshead speed was held at 5 cm/min. All samples were tested at 23°C and 50% relative humidity.

FT-IR transmission spectra of the films were obtained using a Nicolet 5-DX spectrometer with 4 cm^{-1} resolution. Forty interferograms were taken in each case.

The films appeared to be homogeneous, translucent, and pinhole-free by optical microscopic examination.

RESULTS AND DISCUSSION

Thermal Analysis

T_g for pure PnBM is around 20°C[23] and is therefore out of the range over which the DSC scans were taken in this study. A relatively low T_g was desired to avoid producing films that were excessively brittle. T_g vs. Ti oxide content studies will be reported in a future communication. However, significant thermal activity accompanying the release of water, alcohol, and the products of polymer degradation, as well as the evolution of the incorporated Ti oxide phase, however dispersed, is expected. PnBM should degrade to monomer according to the unzipping mechanism[24] and thereby generate a broad endotherm.

Consider, first, the thermal properties of films cast from the 1-3E solutions. DSC scans for these materials are shown in Figure 1. There are two peaks of great endothermal activity in each of these scans, labeled *a* and *d*. While the maximum of peak *a* holds steady at about 75°C, with increasing Ti oxide content, its area increases from 96 to 136 J/g, as listed in Table II. The corresponding

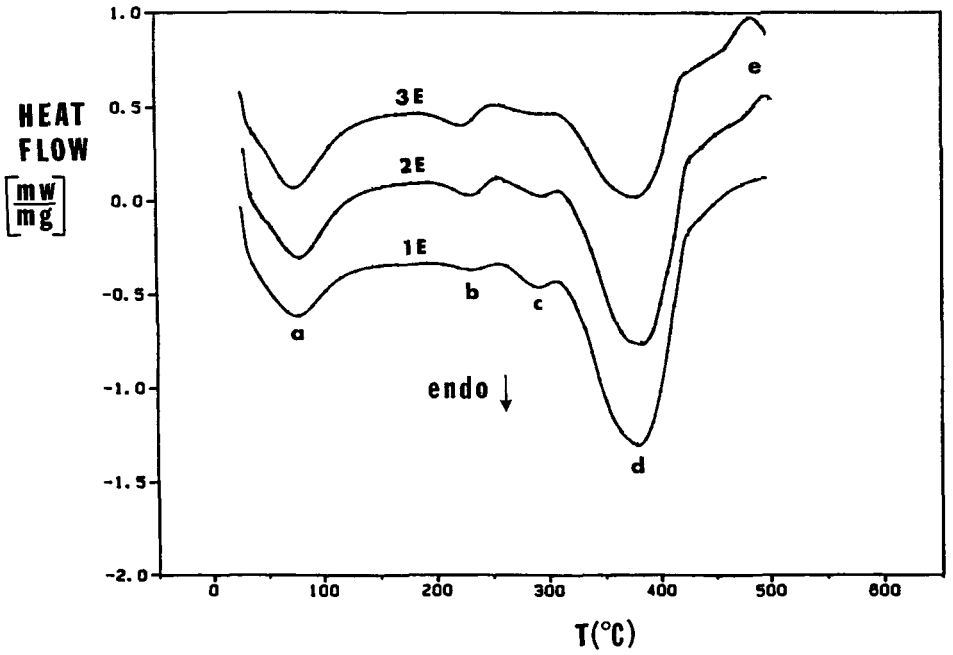

Fig. 1. DSC scans (10°C/min) for PnBM/Ti oxide alloys cast from 1-3E solutions. The 2E and 3E scans have been displaced vertically. Endothermic transitions are labeled *a*, *b*, *c*, and *d* and the exothermic transition, *e*.

TGA scans, seen in Figure 2, show a weight loss in this *a* region attributed to the release of incorporated alcohol and water. We also prepared samples of pure Ti oxide (powders) from TET under conditions identical to those used to

TABLE II
Major Endothermic and Exothermic DSC Peak Temperatures, T_{peak} (°C), and Peak Energies, ΔH (J/g), for Indicated Alloy Compositions, Sol-Gel-Derived Pure TiO_2 Powders, and Pure PnBM

	(*a*)		(*d*)		(*e*)	
Composition	T_{peak}	ΔH	T_{peak}	ΔH	T_{peak}	ΔH
1E	75	96	378	490	None[a]	
2E	76	116	379	429	489	2
3E	75	136	377	375	481	20
TiO_2(TET)	(Endotherm)				(Exotherm)	
	134	715			346	172
1B	55	23	377	477	None[a]	
2B	53	29	376	471	None[a]	
3B	61	47	374	428	None[a]	
TiO_2(TBT)	(Endotherm)				(Exotherm)	
	145	324			None[a]	
PnBM			287	514		

[a] That is, no exotherms observed within investigated temperature range.

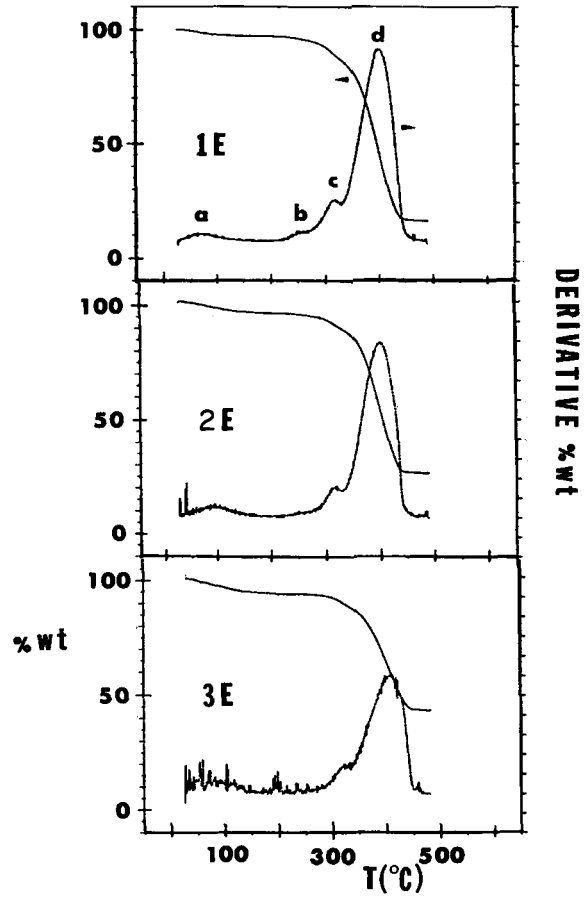

Fig. 2. TGA scans (10°C/min) with corresponding derivative percent weight loss for PnBM/Ti oxide alloys cast from 1-3E solutions. Four significant loss regions are labeled *a*, *b*, *c*, and *d*.

produce the PnBM/Ti oxide films. The one and only weight loss derivative peak for the pure Ti oxide material was in fact centered around the region of peak *a* for the PnBM/Ti oxide films, as seen in Figure 3. Also, the corresponding DSC scan in Figure 3 shows an endothermic peak at a somewhat higher temperature. On the other hand, with reference to Figure 4, films cast from simple PnBM/isopropanol solutions containing neither titanium oxide nor water are seen to have no TGA or appreciable DSC activity in the temperature region of peak *a* for the mixed organic/inorganic system. Therefore, it is quite clear that peak *a* is (1) reflective of the release of alcohol and water and (2) it would seem that these volatiles are more strongly associated with the incorporated Ti oxide rather than the organic phase. This would seem quite reasonable considering the presence of a large number of unreacted polar Ti–OH groups to which water and alcohol molecules could strongly bind in preference to the less polar butyl methacrylate structure.

The DSC scans for films cast from 1-3B solutions are displayed in Figure 5. The profiles in Figures 1 and 5 are qualitatively similar. More specifically, however, the endothermal *a* peaks of Figure 5 occur at lower temperatures than

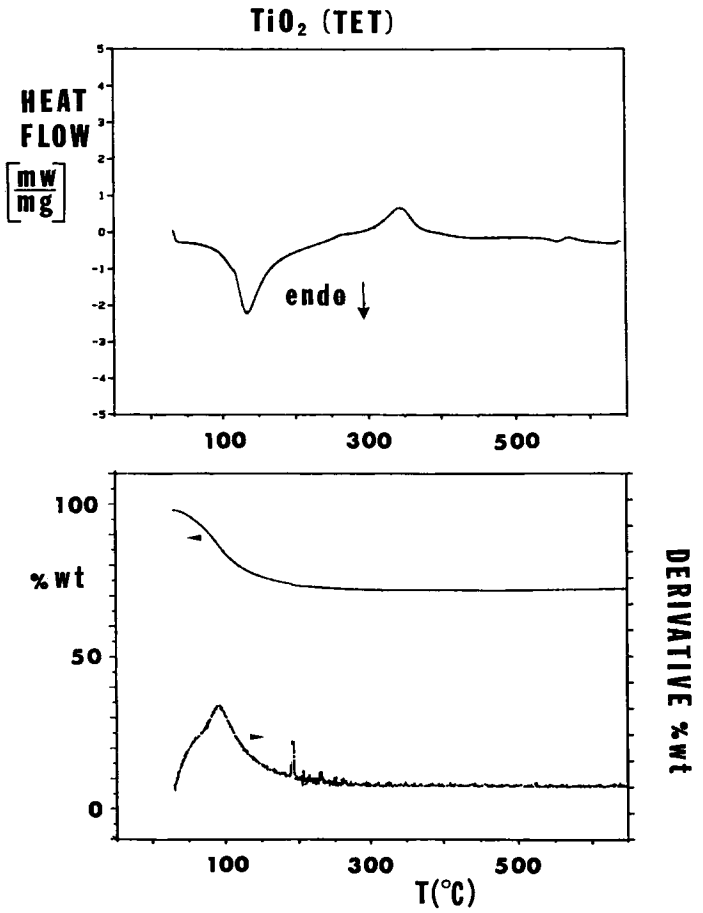

Fig. 3. DSC and TGA scans (both at 10°C/min) for pure TET-derived TiO_2 powder. A non-weight loss exotherm, as well as a weight-loss-accompanied endotherm is seen.

do the *a* peaks of Figure 1 and vary somewhat in position between 53 and 61°C. Moreover, the peak areas are smaller for TBT-derived films, steadily increasing from 23 to 47 J/g with increasing Ti oxide content, as listed in Table II. The corresponding TGA scans in Figure 6 indicate a weight loss in the *a* region again attributed to alcohol–water release. Samples of pure Ti oxide (powders) were prepared by the sol–gel process for TBT under the same conditions as those present in the formulation of the TBT-derived organic/inorganic alloys. A single endotherm whose peak is 11°C higher than, but whose area is only 45% of the area of, the corresponding peak in Figure 3, is seen in Figure 7 along with the parallel TGA scan, which likewise depicts an associated weight loss attributed to the escape of alcohol and water. Actually, despite the difference in DSC peak temperatures and areas, the TGA profiles as well as *onset* of endothermal activities are the same for TET and TBT-derived powders.

Perhaps the fact that the endothermal peak temperature for the pure TBT-derived powders is higher than that for the pure TET-derived powders can be simply rationalized in terms of the boiling points of the alcohols involved. In

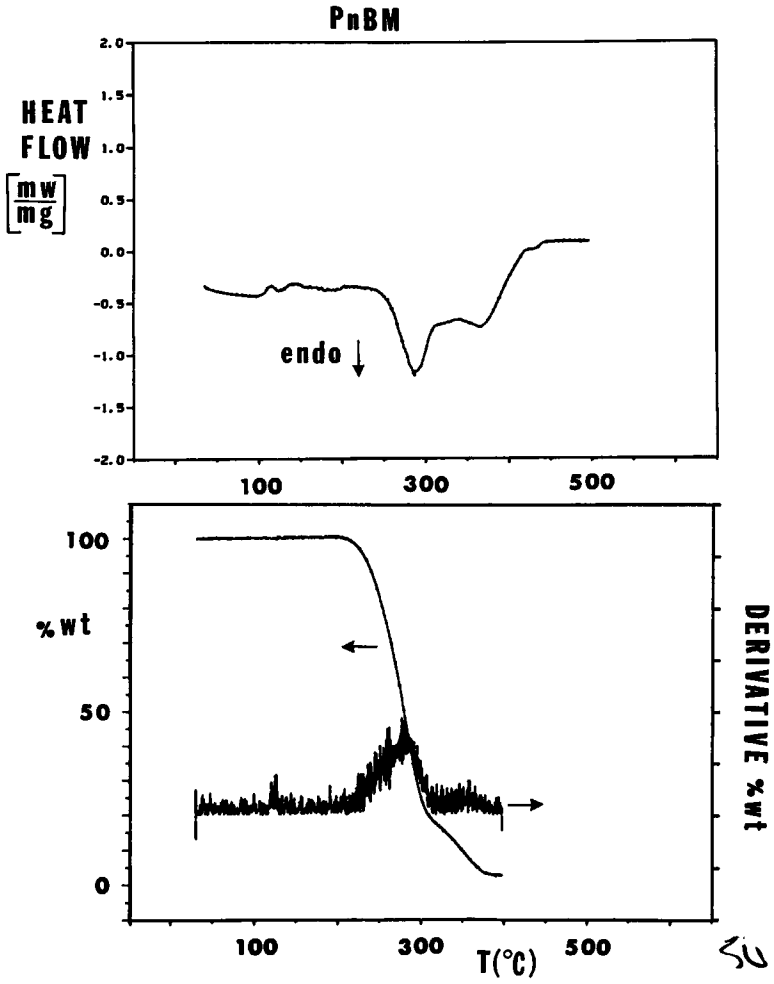

Fig. 4. DSC and TGA scans (both at 10°C/min) for films cast from PnBM/isopropanol solutions. No Ti oxide component is present in these samples.

the course of the sol–gel reaction, considerable relative amounts of ethanol or *n*-butanol are generated. Note in Figure 3 that the (TET-derived) derivative weight loss profile displays a peak near the boiling temperature of water with a distinct shoulder in the region of the boiling points of ethanol (78°C) and isopropanol (83°C). The derivative curve in Figure 7, on the other hand, shows a maximum that reflects isopropanol–water volatilization but lacks the low-temperature shoulder presumably due to the absence of ethanol. *n*-Butyl alcohol, with a boiling point of 118°C, would volatilize to the right of the region of peak water vaporization. In this rough analysis we should, of course, realize that in such a complex mixture the component boiling points will be somewhat depressed each by varying amounts.

The heats of volatile release for the pure TiO_2 powders (TET: 715 J/g, TBT: 324 J/g) are considerably greater than those for the organic/inorganic mixtures basically due to inorganic phase dilution in the latter. We conclude that the

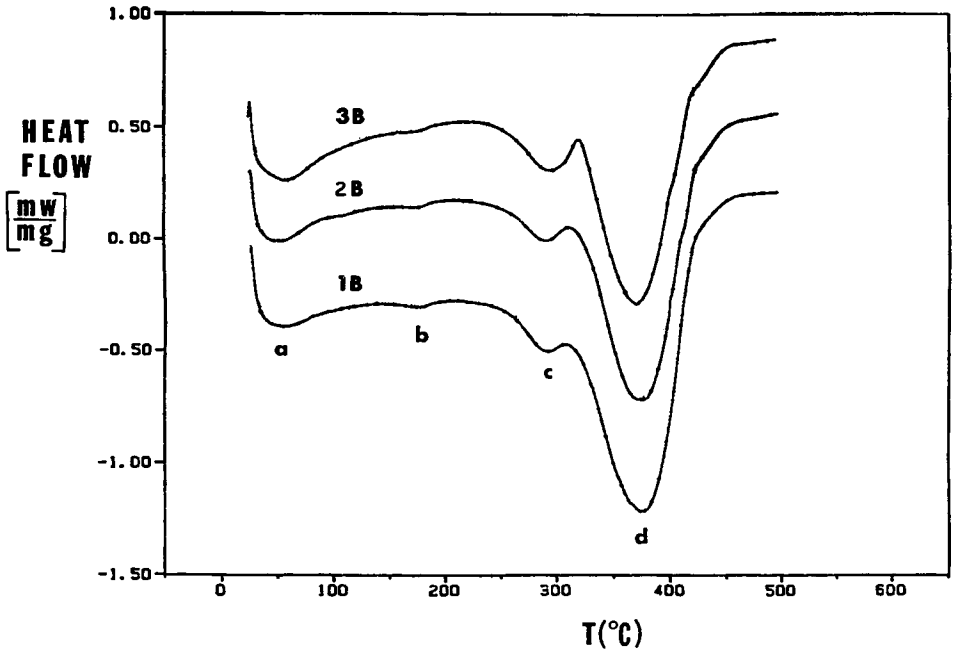

Fig. 5. DSC scans (10°C/min) for PnBM/Ti oxide alloys cast from 1-3B solutions. The 2B and 3B scans have been displaced vertically. Endothermic transitions are labeled *a*, *b*, *c*, and *d*. No exothermic transition is seen within this temperature range.

water and alcohol interacts most strongly with the Ti oxide phase in the mixed systems.

There appear to be two weaker endotherms (peaks *b* and *c*) that precede the largest endotherm (peak *d*) in each of the DSC profiles in Figure 1. Inspection of the corresponding TGA profiles in Figure 2 shows that these peaks are also associated with weight loss. However, the high temperatures at which the weight losses occur as well as the nonoccurrence of calorimetric or thermogravimetric activity of the pure Ti oxide powder at these temperatures (Figure 3) suggests that these transitions are not related to water or alcohol volatilization.

For films cast from 1-3B solutions, similar endotherms are apparent in Figure 5 although peak *b* occurs at a considerably lower temperature than its counterpart in Figure 1. It is seen, with reference to Figure 6, that these peaks are also associated with minor weight loss in the same way as discussed for films cast from the 1-3E solutions.

The largest endotherm in the 1-3E series (peak *d*, Fig. 1) is accompanied by a severe weight loss (Fig. 2). While the peak temperature holds steady at around 378°C, its area steadily decreases from 490 to 375 J/g (Table II) with increasing Ti oxide content. Likewise, the large endotherm in the 1-3B series (peak *d*, Fig. 5) occurs with a great weight loss (Fig. 6) and is slightly shifted from 377 down to 374°C with increasing Ti oxide content. The enthalpies decrease from 477 to 428 J/g (Table II).

The two thermal degradation endotherms and the two accompanying weight losses for the pure PnBM film seen in Figure 4 coincide very well on the temperature axis with peaks *c* and *d* in both Figures 1 and 5. This would suggest

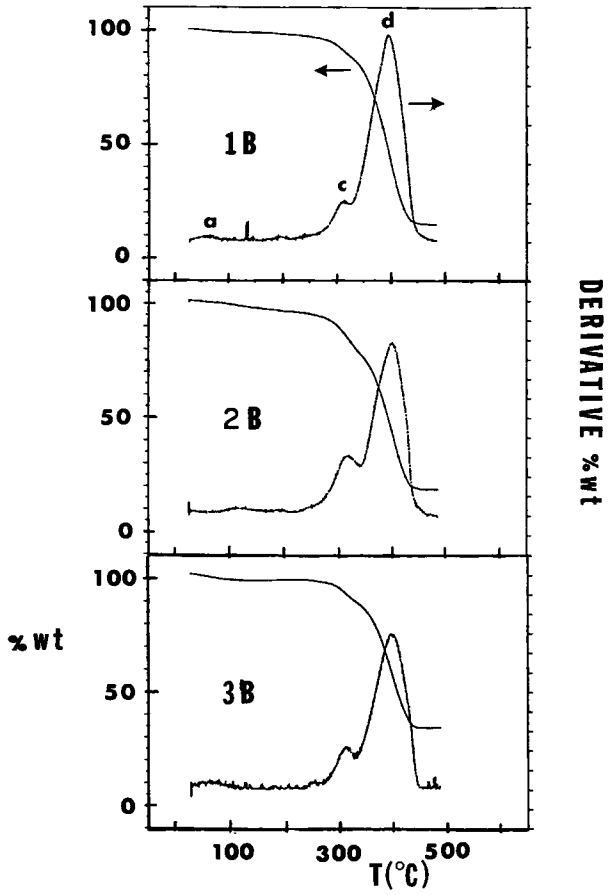

Fig. 6. TGA scans (10°C/min) for PnBM/Ti oxide alloys cast from 1-3B solutions. Three significant weight loss regions are labeled *a*, *c*, and *d*.

that peaks *c* and *d* for films cast from both 1-3E and 1-3B solutions are due to the thermal degradation of the PnBM phase. It would seem that the more massive and more rapid initial degradation event for pure PnBM would correspond to the highly cooperative depolymerization, i.e., unzipping, mechanism. At this time we cannot offer a mechanistic explanation for the slower, less profound but distinct higher temperature degradation process. The fact that the temperatures of these PnBM-related peaks do not shift greatly with composition in the mixed systems would suggest organic/inorganic phase separation, and weak PnBM–Ti oxide intermolecular interactions. We will later discuss the strong tendency of TiO_2 to self-associate due to crystallization as well as our failure to detect appreciable interactions with the C=O group of the PnBM molecules. We note that even when titanium alkoxides are copolymerized with other metal alkoxides, rather than in solution with less interactive organic polymers, microstructural heterogeneity results owing to unequal hydrolysis and condensation reaction rates within and between the two species.[25] Given, then, this phase-separated morphology, the decrease in the *d*-peak areas with increasing Ti oxide content simply is due in most part to the steady decrease

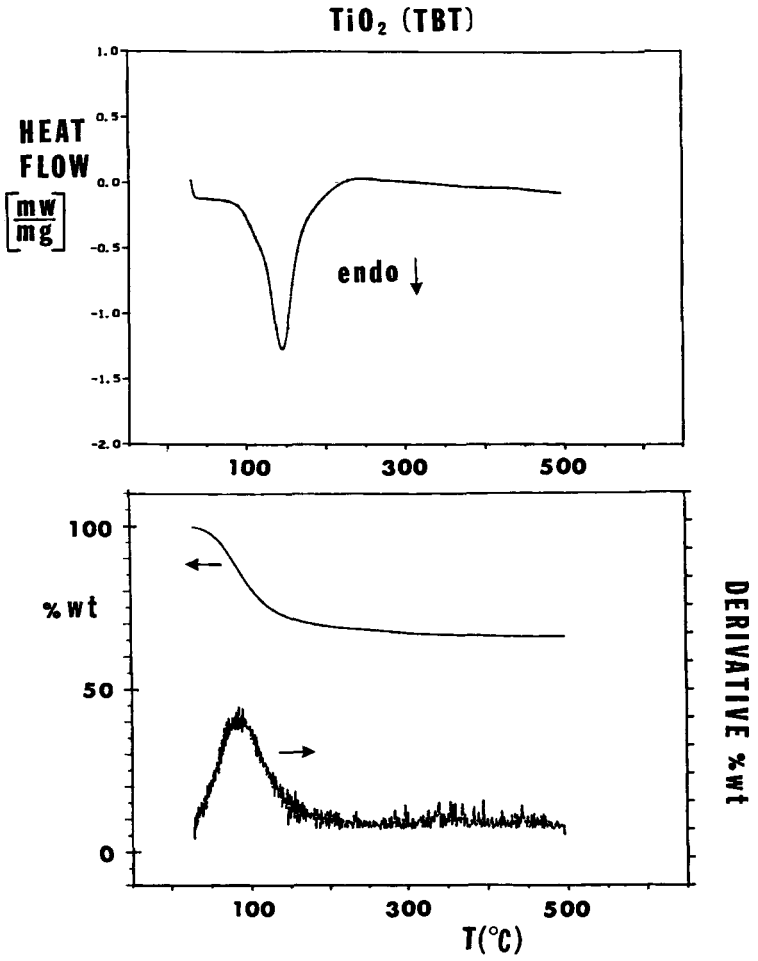

Fig. 7. DSC and TGA scans (both at 10°C/min) for pure TBT-derived TiO_2 powder. In contrast with Figure 3, a high-temperature exotherm is not seen.

in relative organic phase and not to a more complex shift in organic/inorganic molecular interactions within an intimately mixed system.

On the other hand, it is quite significant that the relative magnitudes of these two peaks are reversed in the two mixed systems from their order in pure PnBM. In short, it appears that the major thermal degradation peak temperature for the organic polymer component has been upwardly displaced by around 90°C through the incorporation of the inorganic phase. To be sure, definitive microstructural characterization of these mixed systems is necessary to form a base upon which a rationalization of this interesting and possibly useful modification of PnBM thermal degradation can be built. On an indirect level, we later show that the mechanical tensile characteristics of these materials, especially their ductility, do not seem to indicate that the inorganic (i.e., glassy) component is the load-bearing phase despite its presence in large fraction. If this is the case it would seem that the Ti oxide rather than the rubbery PnBM phase exists in isolation in the sense of not possessing topological connectivity

over macroscopic dimensions. Nonetheless, even if aggregated, the inorganic phase is probably dispersed on a level so fine as to possess a large interfacial surface/volume ratio and thus interact strongly with the PnBM phase so as to modify its thermal degradation behavior as observed.

Lastly, an exothermic peak (*e*) appears at 489°C in the DSC thermogram (Fig. 1) for the film cast from the 2E solution. This peak, having an area of about 2.4 J/g is not visible in the scan for the 1E-derived sample but is enhanced in the scan for the 3E solution-derived film, where the energy has increased to 20 J/g and the peak position has shifted down to 481°C (Table II). There are no weight losses accompanying this exotherm, as seen in Figure 2, and, of course, the organic polymer component appears to have been quite pyrolyzed before this exotherm is reached. We attribute this behavior to *crystallization* of the Ti oxide phase. Water, alcohol, and later unzipped organic polymer repeat units, have been largely driven off by about 450°C. At and beyond this temperature it would seem that there would be considerable molecular mobility within the surviving inorganic phase to allow the network to settle into a minimum energy packing mode with condensation of residual Ti–OH groups with the net result being the observed exotherm. Mukherjee discovered that small anatase crystals can form upon the slow heating of gels derived from titanium isopropoxide at temperatures as low as 350°C.[26] The downward shift in peak temperature might simply be reflective of an increase in ease of crystallization owing to a greater concentration of crystallizable material as seen in Table I. Furthermore, the appearance of this exotherm at the upper edge of the explored temperature range and its increase in magnitude as well as shift to lower temperatures suggests that it may also exist for 1E solution-derived samples but simply occurs at a temperature higher than those explored.

An inspection of Figure 3 reveals an exothermal peak at 346°C for the pure TET-derived titania powder with no weight loss. This exotherm is quite within the vicinity of the aforementioned anatase crystallization temperature of Mukherjee but is considerably lower in temperature but greatly higher in energy/mass than the exotherm for the mixed system in Figure 1. We might rationalize the retardation of crystallization within the mixed system by referring to Figure 2 on which it appears that organic material persists and might serve to disperse the inorganic phase up to about 450°C. After the organic "defects" have been volatilized, crystallization can proceed unhindered. Indeed the material having the least amount of PnBM displays the lower exothermal peak temperature.

On the other hand, with reference to Figure 5, no exotherm was detected for any PnBM/Ti oxide composition for the TBT-derived materials over the temperature range of DSC investigation. Furthermore, no exotherm is seen in Figure 7 for the pure TBT-derived titania powders. Therefore, the absence of a thermally induced crystalline transformation in the TBT-derived mixed system would seem to be due to the intrinsic hydrolysis and condensation characteristics of this particular alkoxide independent of its incorporation within the organic polymer environment. Berglund et al. performed a Raman spectroscopic analysis of the kinetics of the hydrolysis of titanium isopropoxide.[27] Solutions having initial H_2O/Ti ratios of 1.0, 2.0, and 2.8, while displaying rapid initial hydrolysis, showed a subsequent slowing of the reaction and incomplete hydrolysis at long times. Perhaps the even lower reactivity of the larger butoxyl group might prevent the ultimate formation of crystalline order.

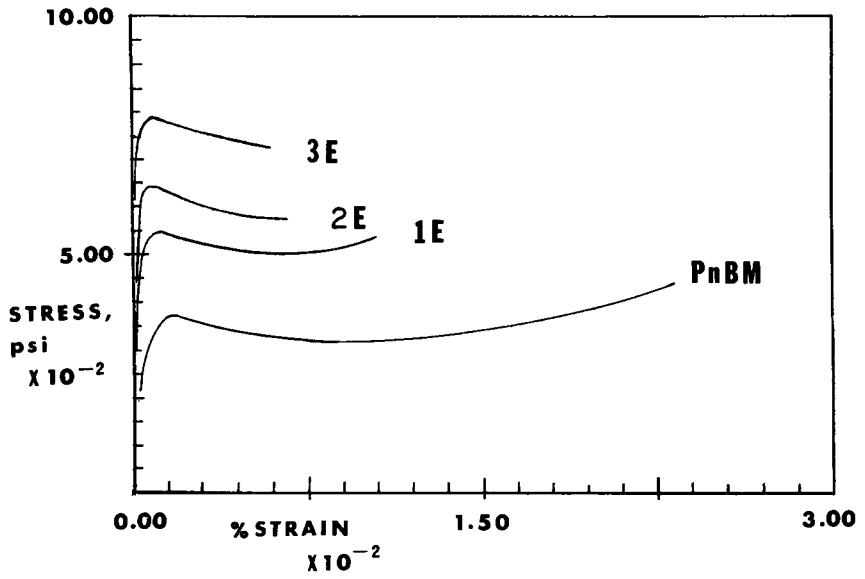

Fig. 8. Mechanical tensile stress vs. strain for PnBM/Ti oxide alloys cast from 1-3E solutions and for pure solution-cast PnBM.

Mechanical Tensile Studies

The tensile stress vs. strain characteristics of alloys derived from 1-3E solutions, along with the curve for solution-cast pure PnBM for comparison, are displayed in Figure 8. It is rather evident that these hybrid materials acquire an increase in Young's modulus, quantitatively represented in Figure 9, and

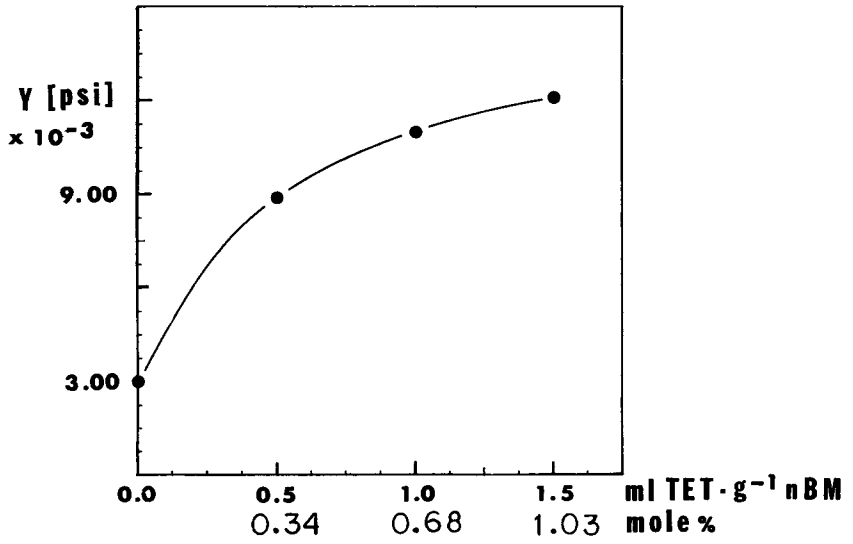

Fig. 9. Young's modulus, from stress–strain curves, vs. Ti oxide content for PnBM/Ti oxide alloys derived from 1-3E solutions.

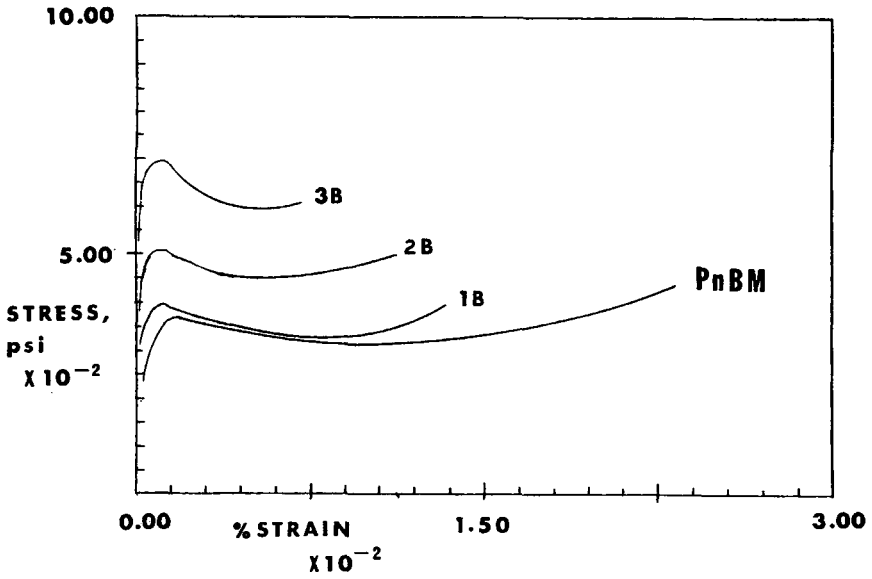

Fig. 10. Mechanical tensile stress vs. strain for PnBM/Ti oxide alloys cast from 1-3B solutions and for pure solution-cast PnBM.

an increase in tensile strength, as well as a decrease in ductility, all in controlled monotonic fashion with increasing Ti oxide content.

The same general behavior is seen for films cast from 1-3B solutions as shown in Figures 10 and 11. On closer inspection, however, it appears that the samples in the E series are more strengthened than their counterparts in the

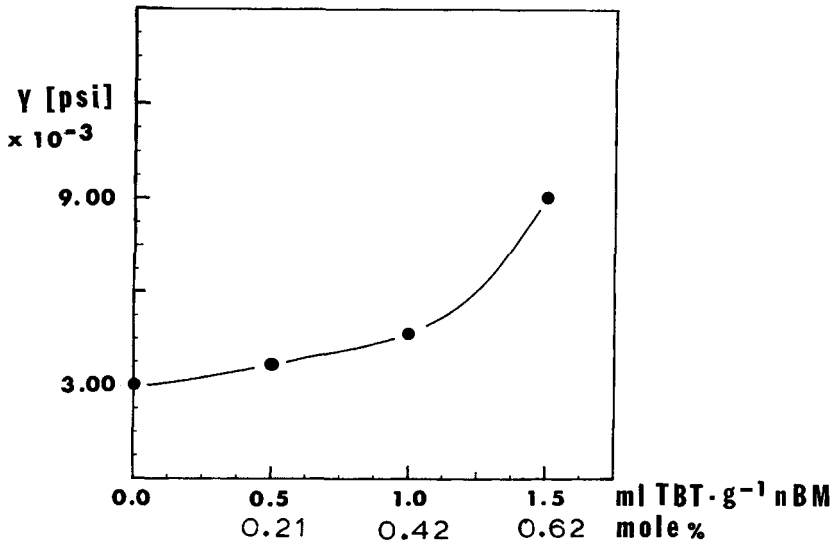

Fig. 11. Young's modulus, from stress–strain curves vs. Ti oxide content for PnBM/Ti oxide alloys derived from 1-3B solutions.

B series, although it should be remembered that a given B solution has a lower titanate/PnBM mole ratio than its corresponding E solution. Also, the modulus vs. Ti oxide content curves are concave downward for the E series but are concave upward for the B series. The only film exhibiting any weaker mechanical tensile parameter than those of the pure PnBM samples was that issuing from the 1B solution for which the ultimate tensile strength was about 10% lower.

To be sure, a detailed microstructural analysis is required before the compositional trends for mechanical tensile properties, or any properties for that matter, can be rationalized without ambiguity. The geometry and topology (connectivity) of organic/inorganic microphase separation, the degree of branching and crosslinking within the invasive metal oxide phase and nature and degree of interphase interactions are clearly of utmost importance.

Let us at least digress at this time to review some basic salient facts that have been established for sol–gel-derived TiO_2 materials.

Ti alkoxides hydrolyze more vigorously with water[28,29] than do the Si alkoxides as utilized in our earlier efforts to produce perfluoro-ionomer/Si oxide microcomposites.[13–15] In dilute solutions, when the $H_2O/Ti(OR)_4$ mole ratio is less than one, such as would occur upon exposure to water vapor, essentially linear polymers containing at most some branches but no crosslinking are formed.[28] In our case we might expect the reactants to continue to be diluted to some degree by the polymer even after the volatiles have been removed. Of course, while the components in the initial solutions were mixed on the molecular level, the subsequently formed orthotitanic acid molecules and oligomers will be more polar than their alkoxide precursors, which would render PnBM–titanate interactions less favorable. Add to this the crystallization tendency for titanates as well as its presence in high composition, and one might reasonably expect aggregation to occur to some degree. Polycondensation is slower for larger alkyl groups for steric reasons.[30] For this reason, perhaps, the E series may possess Ti oxide phases that are more invasive than the inorganic phases in corresponding samples of the B series, although we must again bear in mind that compositions are comparatively lower in the B series. Mechanical stresses would therefore be transferred more efficiently throughout the better-reinforced structures of the E series of alloys. Certainly, a presently unaccountable complication to the overall reaction scheme might be that of transesterification, that is, an ester interchange reaction of a higher alcohol solvent with lower alkyl orthotitanates.

In contrast with tetraethoxy-or-methoxysilane, the polymerization of titanium alkoxides is known to proceed with crystallization although amorphous gels are said to be affected with water added in less than stoichiometric amounts.[30] In any case, the anatase crystal form can be induced upon drying. It is interesting to note that Huckel, referring to conventional processing methods at an earlier time, stated that TiO_2 does not form a glass.[31] It is also stated that the anatase structure cannot be formed from pure TiO_2 melts but does arise in microcrystalline form from hydrated titanium dioxide issuing from the hydrolysis of titanium compounds.[32]

We note, on inspection of Figures 8 and 10, that our materials remain ductile, although increasingly less so, with increasing Ti oxide content. A manifestation of the onset of brittleness would most likely signal one of the following two situations: (1) an inorganic phase that begins to span macroscopic dimensions

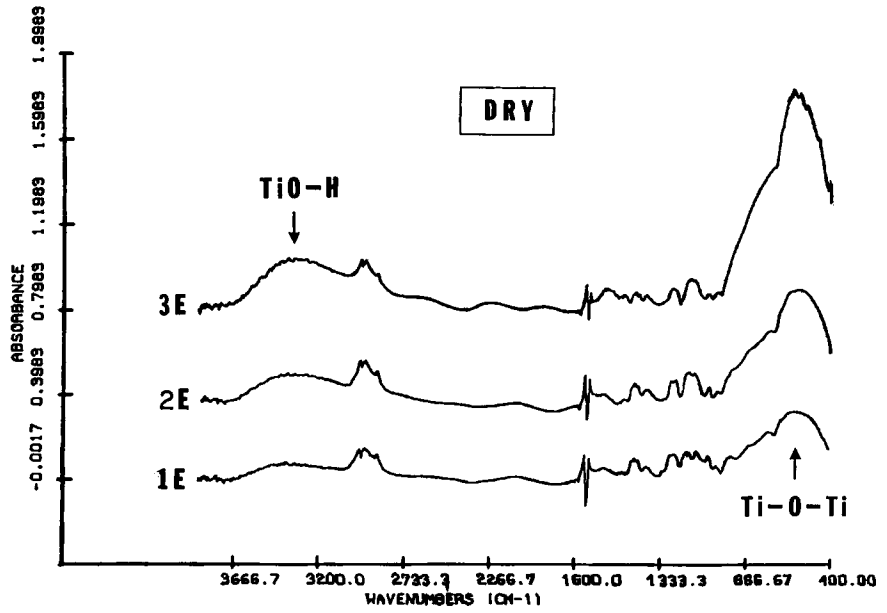

Fig. 12. FT-IR difference spectra for dried PnBM/Ti oxide alloy films cast from 1-3E solutions. The 2E and 3E scans have been displaced vertically. The positions of the TiO–H and Ti–O–Ti vibrations in the inorganic phase are indicated.

and in effect becomes the major load-bearing component or (2) a PnBM chain segmental mobility that is progressively restricted by the inorganic phase so as to raise the polymer's T_g above ambient temperature.

At this time we are inclined to believe that the mechanical tensile response supports the view that the inorganic phase is discontinuous but nonetheless serves to immobilize the polymer chains but not in the manner of simple chemical crosslinks in a well-defined network. For example, it is seen in Figures 9 and 11 that the quantity $Y/3RT$ = crosslink density (for an ideal network) is not directly proportional to the actual average concentration of incorporated Ti oxide. Furthermore, as earlier noted, the curvatures of these graphs are in the opposite sense for the two initial alkoxides. To be sure, subambient DSC studies of T_g vs. composition are needed to clarify the issue of the restriction of PnBM chain segmental mobility by the inorganic phase.

Infrared Spectroscopy

Infrared spectroscopic studies of pure TiO_2 powders produced by the sol–gel reaction for TET where H_2O : TET = 2 : 1 indicate a very strong absorbance around 600 cm^{-1}.[33] Pure anatase also has a strong peak at around 660 cm^{-1}.[34] Oligomers of condensed TBT have IR peaks at 820(s) and 763(m) cm^{-1} due to Ti–O–Ti bonds.[35] It is reasonable to think that these oligomeric vibrations might shift to lower wave numbers with increasing molecular mass. It has also been stated that an absorption band at 960 cm^{-1} indicates fourfold coordination about the Ti atoms.[36] The previously mentioned TiO_2 powders (which were heated at 500°C) do in fact exhibit a weak peak at this position, but samples

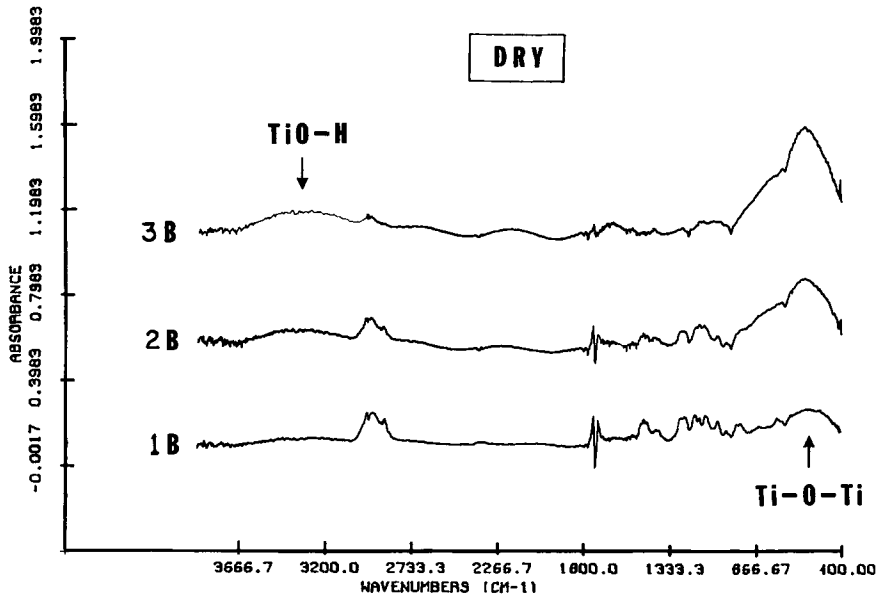

Fig. 13. FT-IR difference spectra for dried PnBM/Ti oxide alloy films cast from 1-3B solutions. The 2B and 3B scans have been displaced vertically. The positions of the TiO–H and Ti–O–Ti vibrations in the inorganic phase are indicated.

for which H_2O : TET = 15 : 1 do not. All three crystal forms of TiO_2—rutile, anatase, and brookite—consist of Ti atoms that are surrounded by six oxygen atoms in rather symmetric *octahedral* coordination. On the other hand, the threefold symmetry of coordination of Ti atoms about oxygen atoms must not only be quite variable to account for the observed crystal polymorphism but also must be responsible for the allowance of the glassy structures referred to earlier.[30] We note that the IR spectrum of anatase in fact contains no evidence of the cited tetrahedrally related band in the vicinity of 960 cm^{-1}.

A reference spectrum of pure PnBM was obtained from a dried thin film cast from isopropanol solution. We chose to subtract the PnBM contribution from the mixed system spectra by subtracting the pure PnBM spectrum using the carbonyl peak at 1720 cm^{-1} as an internal thickness standard. While the resultant subtractions were not complete, the Ti oxide bands were significantly enhanced in this way.

Difference spectra for the 1-3E and 1-3B series of films are shown in Figures 12 and 13, respectively. The imperfect subtraction is given evidence by the persistence of three closely spaced PnBM peaks at slightly less than 3000 cm^{-1}.

As the samples have been well dried, the progressive increase in the broad absorbance at around 3500 cm^{-1}, with increasing Ti oxide concentration, can be reasonably attributed to the OH vibration in uncondensed Ti–OH groups that exist in a wide distribution of molecular environments.

There is a strong and broad absorption peak from about 650 to 400 cm^{-1} that increases in relative magnitude with increasing Ti oxide concentration. Based on the earlier-cited vibrational assignments for similar systems, we believe that this is a region that is accounted for by vibrations of the Ti–O–Ti grouping

as also existing within a broad spectrum of local environments. Included within the general concept of molecular heterogeneity would be varying states of Ti substitution on the nearest-neighbor oxygens that coordinate about a given Ti atom, i.e., degree of chain branching within the invasive inorganic network. To be sure, the strength of the TiO–H peak relative to that of the Ti–O–Ti peak suggests that the Ti oxide phase is not highly condensed, or interconnected, in a molecular network sense.

The spectra of undried films (e.g., see Fig. 14), of course, show greater absorbance in the OH stretching region owing to the presence of water and alcohol. The bending mode of H_2O (ca. 1620 cm^{-1}) seen in Figure 14 is essentially imperceptible in the spectra of the dry samples. In all samples, wet and dry, at all Ti oxide concentrations, a shoulder appears on the high wave number side of the Ti–O–Ti peak. While we cannot provide a definite interpretation of this prominent discrete shoulder, it is nonetheless tempting to think of this as a possible manifestation of tetrahedral vs. octahedral coordination about Ti atoms, as discussed earlier.

Lastly, one might consider the possibility of having strong organic/inorganic interphase interactions of the following nature: Ti–O–H---O=C. However, as no shift in the PnBM carbonyl frequency was detected, we might conclude that such interactions are not appreciable.

GENERAL CONCLUSIONS

A successful but simple method has been developed to cast novel organic/inorganic hybrid films from multicomponent solutions containing titanium alkoxides (ethyl, *n*-butyl), poly(*n*-butyl methacrylate), water, and isopropanol of prescribed compositions. The ensuing sol–gel reaction for both alkoxides and subsequent controlled drying procedure results in materials of mechanical integrity for which the multistep thermal degradation profile of the organic

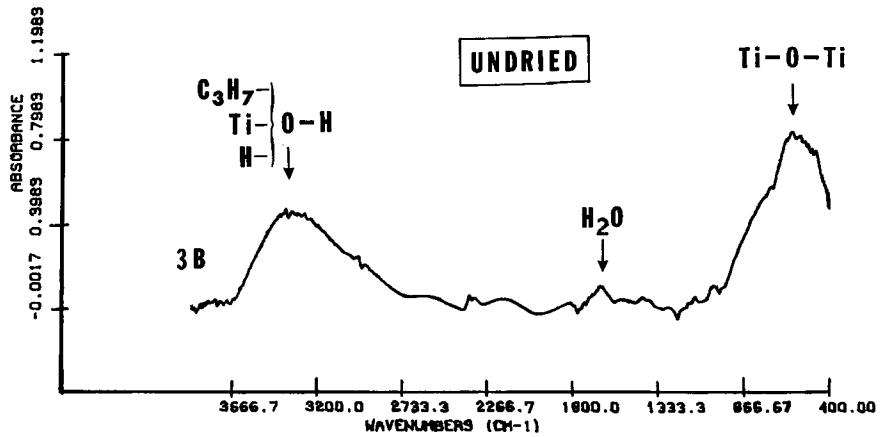

Fig. 14. FT-IR difference spectrum for an undried PnBM/Ti oxide alloy film cast from a 3B solution. The positions of various unresolved O–H vibrations, the bending vibration of H_2O and the Ti–O–Ti vibrations are indicated.

polymer has been significantly modified so as to retard the onset of the major weight loss event. On heating and prior to degradation it appears that residual alcohol/water is released as if these incorporated volatiles were distinctly bound by the more polar Ti oxide phase. It is suggested that the general concept of organic/inorganic phase separation within these materials is in harmony with their observed thermal behavior.

A crystallization exotherm, presumably due to anatase formation, is present in DSC scans for the TET-, but not TBT-derived films. While this crystalline transformation takes place beyond polymer degradation temperatures, the general concept nonetheless might be useful within the realm of tailoring ceramic precursor materials in which the organic phase is considered to be sacrificial in any case.

The trend of mechanical tensile parameters with increasing Ti oxide content using both TET and TBT alkoxide precursors depicts a material that is progressively strengthened. We are presently of the opinion that these mechanical studies indirectly indicate that the Ti oxide phase, while being aggregated and providing material reinforcement, is discontinuous over macroscopic dimensions and that the PnBM phase does not exist as a crosslinked network in the traditional sense.[37]

FT-IR subtraction spectra of these films only depict rather general characteristics of the Ti oxide phase: (1) a significant relative number of unreacted OH groups and their distribution over a broad range of molecular environment; (2) a very broad spectrum of molecular environments adjacent to Ti–O–Ti bridges that is likewise, in the main, due to incomplete polyfunctional condensation. In short, we feel that the IR spectra are reflective of an invasive Ti oxide network that is not highly interconnected.

We would like to stress that these studies were of an exploratory nature and regard our interpretations as tentative, pending further critical structural characterization. Our suggestions at this time are mainly intended to form an hypothetical basis for future experimental design of these interesting and unique organic/inorganic hybrid materials.

Acknowledgment is make to the donors of the Petroleum Research Fund, administered by the American Chemical Society, and the Plastics Institute of America for support of this research.

References

1. B. E. Yoldas, *J. Mater. Sci.*, **12**, 1203 (1977); **14**, 1843 (1979).
2. M. Yamane, S. Aso, and T. Sakaino, *J. Mater. Sci.*, **13**, 865 (1978).
3. S. P. Mukherjee, *J. Non-Crystall. Solids*, **42**, 477 (1980).
4. R. Aelion, A. Loebel, and F. Eirich, *J. Am. Chem. Soc.*, **72**, 5705 (1950).
5. B. E. Yoldas, *J. Mater. Sci.*, **10**, 1856 (1975).
6. R. M. Brick and A. Phillips, *Structure and Properties of Alloys*, McGraw-Hill, New York, 1949, Chapter 3.
7. S. J. Clarson and J. E. Mark, *Polym. Comm.*, **28**, 249 (1987), and numerous references therein.
8. W. Noll, *The Chemistry and Technology of Silicones*, Academic Press, New York, 1968.
9. E. L. Warrick, O. R. Pierce, K. E. Polmanteer, and J. C. Saam, *Rubber Chem. Technol.*, **52**, 437 (1979).
10. Y.-P. Ning, M.-Y. Tang, C.-Y. Jiang, J. E. Mark, and W. C. Roth, *J. Appl. Polym. Sci.*, **29**, 3209 (1984).

11. J. E. Mark, in *Science of Ceramic Chemical Processing,* L. L. Hench and D. R. Ulrich, Eds., Wiley, New York, 1986, p. 434.

12. J. E. Mark, *Rubber Chem. Technol.,* **48,** 495 (1975).

13. K. A. Mauritz, C. K. Jones, and R. F. Storey, *Am. Chem. Soc. PMSE Preprints,* **85,** 1079 (1988).

14. K. A. Mauritz, R. F. Storey, and C. K. Jones, in *Multiphase Polymer Materials: Blends, Ionomers and Interpenetrating Networks,* L. A. Utracki and R. A. Weiss, Eds., ACS Symp. Ser., Amer. Chem. Soc., Wash., D.C., **395** (1989).

15. K. A. Mauritz and R. M. Warren, *Macromolecules,* **22,** 1730 (1989).

16. G. L. Wilkes, H. Huang, and R. H. Glaser, *ACS Symp. Ser. Advan. Silicon-Based Polym. Sci.,* to appear.

17. H. Huang, R. H. Glaser, and G. L. Wilkes, *ACS Symp. Ser.,* **360,** 354 (1987).

18. R. H. Glaser and G. L. Wilkes, *Polym. Bull.,* to appear.

19. G. L. Wilkes, B. Orler, and H. Huang, *Polym. Prep.,* **26**(2), 300 (1985).

20. H. Huang, B. Orler, and G. L. Wilkes, *Polym. Bull.,* **14**(6), 557 (1985).

21. H. Huang, R. H. Glaser, and G. L. Wilkes, *Polym. Prep.,* **28**(1), 434 (1987).

22. H. Huang, B. Orler, and G. L. Wilkes, *Macromolecules,* **20**(6), 1322 (1987).

23. J. Brandrup and E. H. Immergut, Eds., *Polymer Handbook,* 2nd ed., Wiley, New York, 1975, p. III-147.

24. E. M. Pearce, C. E. Wright, and B. K. Bordoloi, *Laboratory Experiments in Polymer Synthesis and Characterization,* EMMSE Project, Penn. State U., 1982, p. 275.

25. W. C. LaCourse and S. Kim in *Science of Ceramic Chemical Processing,* L. L. Hench and D. R. Ulrich, Eds., Wiley, New York, 1986, p. 304.

26. S. Mukherjee, in *Emergent Process Methods for High Technology Ceramics,* R. F. Davis, H. Palmour, and R. L. Porter, Eds., Plenum, New York, 1984, pp. 95–110.

27. K. A. Berglund, D. R. Tallant, and R. G. Dosch, in *Science of Ceramic Chemical Processing,* L. L. Hench and D. R. Ulrich, Eds., Wiley, New York, 1986, p. 94.

28. T. Boyd, *J. Polym. Sci.,* **7**(6), 591 (1951).

29. C. C. Bradley, R. Gaze, and W. Wardlaw, *J. Chem. Soc.,* **4,** 3977 (1955).

30. M. Prassas and L. L. Hench, in *Ultrastructure Processing of Ceramics, Glasses and Composites,* L. L. Hench and D. R. Ulrich, Eds., Wiley, New York, 1984, p. 108.

31. W. Huckel, *Structural Chemistry of Inorganic Compounds,* Elsevier, Amsterdam, 1951, Vol. II, p. 679.

32. H. B. Weiser and W. O. Milligan, *J. Phys. Chem.,* **38,** 513 (1934).

33. B. E. Yoldas, in *Ultrastructure Processing of Ceramics, Glasses and Composites,* L. L. Hench and D. R. Ulrich, Eds., Wiley, New York, 1984, p. 65.

34. *An Infrared Spectroscopy Atlas for the Coatings Industry,* Federation Soc. Coatings Technol., IR Spectr. Committee, J. T. Vandeberg, Chmn., Philadelphia, 1980, spectrum 825.

35. V. A. Zeitler and C. A. Brown, *J. Phys. Chem.,* **61,** 1174 (1957).

36. S. V. Lysak and B. Ya., *Sukharevskii Doklad Arad Nauk SSSR,* **188,** 1295 (1969).

37. P. J. Flory, *Principles of Polymer Chemistry,* Cornell University Press, Ithaca, 1953, Chapters 9 and 11.

Received January 13, 1989
Accepted June 8, 1989